

Production of $\gamma\gamma + 2$ jets from double parton scattering in proton-proton collisions at the LHC ^{*}

TAO Jun-Quan^{1,1)} ZHANG Si-Jing^{1,2} SHEN Yu-Qiao^{1,2}
FAN Jia-Wei^{1,2} CHEN Guo-Ming¹ CHEN He-Sheng¹

¹ Institute of High Energy Physics, Chinese Academy of Sciences, Beijing 100049, China

² University of Chinese Academy of Sciences, Beijing 100049, China

Abstract: Cross sections for the production of pairs of photons plus two additional jets produced from double parton scattering in high-energy proton-proton collisions at the LHC are calculated for the first time. The estimates are based on the theoretical perturbative QCD predictions for the productions of $\gamma\gamma$ at next-to-next-to-leading-order, jet + jet and γ + jet at next-to-leading-order, for their corresponding single-scattering cross sections. The cross sections and expected event rates for $\gamma\gamma + 2$ jets from double parton scattering, after typical acceptance and selections, are given for proton-proton collisions with the collision energy $\sqrt{s} = 13$ TeV and an integrated luminosity of 100 fb^{-1} planned for the following two years, and also $\sqrt{s} = 14$ TeV with 3000 fb^{-1} of integrated luminosity as LHC designed.

Key words: $\gamma\gamma + 2$ jets production, double parton scattering, QCD

PACS: 11.80.La, 12.38.Bx, 25.20.Lj

1 Introduction

In proton-proton (pp) collisions with higher energies at the Large Hadron Collider (LHC), particle production is dominated by multiple interactions of their constituent partons, with most particles from the hardest proton-proton scattering and the radiation and fragmentation of secondary partonic actions. The higher centre-of-mass energy leads to enhanced parton densities which cause a sizable probability for two or more parton-parton scatterings within the same pp interaction [1, 2]. At LHC, various measurements of the differential distributions in W + jets [3, 4] and J/ψ + W [5] show that the excesses above the expectations from single parton scattering (SPS) are consistent with double parton scattering (DPS). Various measurements in other pp and $p\bar{p}$ collisions at $\sqrt{s} = 63$ GeV [6], 630 GeV [7], and 1.8 TeV [8] are consistent with DPS contributions to multijet final states, as well as to γ + 3-jet events at $\sqrt{s} = 1.8$ TeV [9] and 1.96 TeV [10]. The measurements of DPS processes can provide valuable information on the transverse distribution of partons in the proton [11] and on the multi-parton correlations in the hadronic wave function [12]. DPS also constitutes the background for new physics searches at the LHC [13–15]. Additional searches for DPS have been proposed via double Drell-Yan, four jets and same-sign WW production [16–18].

In this paper, the cross section for the production of pairs of photons plus two additional jets produced from

double parton scattering (DPS) in high-energy proton-proton collisions at the LHC are calculated for the first time. $\gamma\gamma$ final states have played a crucial role in the recent discovery of a new boson at the LHC [19, 20] and are also important in many New Physics searches [21–24], in particular the search for extra spatial dimensions or cascade decays of heavy new particles. In particular, diphotons in combination with jets and missing energy occur in gauge mediated SUSY scenarios. $\gamma\gamma$ or plus two additional jets offers also an important test of both perturbative and non-perturbative quantum chromodynamics (QCD) [25–27]. $\gamma\gamma + 2$ jets is also the main irreducible background for other physics analyses with $\gamma\gamma$ and jets in the final state at the LHC, such as Higgs produced in vector boson fusion. For the production of $\gamma\gamma + 2$ jets, a sizeable contribution from DPS with $\gamma\gamma$ produce in one scattering while the second scattering yielding two jets can be expected.

The structure of this paper is organized as follows. In section 2, a generic way of the DPS cross section as the product of the SPS cross sections and its parameter are briefly introduced. The details of the cross section of $\gamma\gamma + 2$ jets calculation and the cross section of different SPS processes estimated from higher order theoretical predictions are described in section 3. The results including the cross section of $\gamma\gamma + 2$ jets with $\sqrt{s} = 13$ TeV and 14 TeV at LHC and the expected event rates, with typical selections, are summarized in section 4. The summary and outlook are given in section 5.

^{*} Supported by National Natural Science Foundation of China (No. 11061140514), China Ministry of Science and Technology (No. 2013CB838700) and in part by the CAS Center for Excellence in Particle Physics (CCEPP)

1) E-mail: taojq@mail.ihep.ac.cn

2 Generic formule of DPS

For a composite system ($A+B$) in hadronic collisions, its production cross section from DPS, $\sigma_{pp \rightarrow AB}^{DPS}$, can be written model-independently as the product of the cross sections of A and B originated from single parton scattering, $\sigma_{pp \rightarrow A}^{SPS}$ and $\sigma_{pp \rightarrow B}^{SPS}$, normalized by an effective cross section σ_{eff} [28]

$$\sigma_{pp \rightarrow AB}^{DPS} = \frac{m}{2} \frac{\sigma_{pp \rightarrow A}^{SPS} \times \sigma_{pp \rightarrow B}^{SPS}}{\sigma_{eff}}, \quad (1)$$

where m is a symmetry factor accounting for distinguishable ($m=2$) and indistinguishable ($m=1$) final-states.

The effective cross section σ_{eff} is a measure of the transverse distribution of partons inside the colliding hadrons and their overlap in a collision. It is independent of the process and of the phase-space under consideration. A number of measurements of σ_{eff} have been performed in pp and $p\bar{p}$ collisions at $\sqrt{s} = 63$ GeV [6], 630 GeV [7], 1.8 TeV [8, 9, 29], 1.96 TeV [10] and also 7 TeV at LHC [3, 4]. The measured values range from 5mb at the lowest energy to about 20mb from CMS at 7 TeV. Fig. 1 shows a comparison of the effective cross section σ_{eff} measured by different experiments using different processes at various centre-of-mass energies.

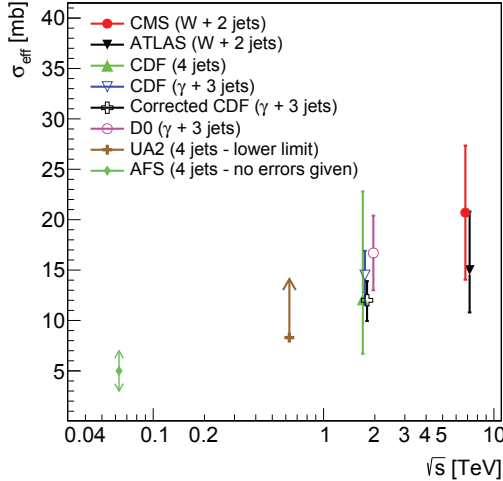


Fig. 1. σ_{eff} measured by different experiments using different processes [3, 4, 6–10, 29]. The "Corrected CDF" data point indicate the σ_{eff} value corrected for the exclusive event selection [29].

The measured values of σ_{eff} from TeV experiments at Tevetron (CDF and D0) and LHC (ATLAS and CMS) are consistent with each other within their uncertainties. In the following calculations, a numerical value $\sigma_{eff} \approx 15$ mb was used to estimate the production cross section of

$\gamma\gamma + 2$ jets from DPS with $\sqrt{s} = 13$ TeV and 14 TeV at LHC. A number 5 mb was assigned as its uncertainty to estimate its effects on the final results. The uncertainty on σ_{eff} is the dominant uncertainty for the calculation of the production cross section of $\gamma\gamma + 2$ jets from DPS in the following sections

3 $\sigma_{pp \rightarrow \gamma\gamma+2jets}^{DPS}$ calculation

According to the description in above section, the production cross section of $\gamma\gamma + 2$ jets from DPS in pp collisions can be written as

$$\sigma_{pp \rightarrow \gamma\gamma+2jets}^{DPS} = \frac{\sigma_{pp \rightarrow \gamma\gamma}^{SPS} \times \sigma_{pp \rightarrow 2jets}^{SPS}}{\sigma_{eff}} + \frac{1}{2} \frac{\sigma_{pp \rightarrow \gamma+jet}^{SPS} \times \sigma_{pp \rightarrow \gamma+jet}^{SPS}}{\sigma_{eff}}. \quad (2)$$

$\gamma\gamma$ production has been calculated at next-to-leading-order (NLO) some time ago [30], supplemented also by gluon initiated subprocesses beyond the leading order [31] and soft gluon resummation [32, 33]. Recently, next-to-next-to-leading-order (NNLO) corrections to direct diphoton production also have become available [34]. The measurements from LHC [25–27] show that the NNLO can give much better agreement with measured data than the lower order predictions. For the integrated cross section, the predicted values by NNLO are almost exactly the same [27] or consistent within the uncertainties [25, 26] with the measured ones. So for the production cross sections of $\gamma\gamma$ final-state from SPS, $\sigma_{pp \rightarrow \gamma\gamma}^{SPS}$, with different \sqrt{s} will be obtained from the NNLO calculation with the package 2 γ NNLO.

For the dijet cross section, the measured data at LHC [35, 36] can be well described by NLO perturbative QCD (pQCD) calculations from NLOJet++ program [37] corrected to account for non-perturbative and electroweak effects. From [35], the non-perturbative correction is within 3% for jet reconstructed with the anti- k_t clustering algorithm [38] and distance parameter or cone size $R=0.4$. The corrections for the electroweak effect can be negligible if the dijet mass less than about 1 TeV. In this analysis, the NLO calculations of $\sigma_{pp \rightarrow 2jets}^{SPS}$ are performed using NLOJet++ (version 4.1.3) within the framework of the fastNLO package (version 2.3.1) [39].

NLO pQCD prediction from the program JETPHOX (version 1.3.1) [40] is used for the calculation of $\gamma + jet$ cross sections from SPS in this paper. This program includes a full NLO QCD calculation of both the direct-photon and fragmentation contributions to the cross section. The number of flavours was set to five. Compared with the measurements of $\gamma + jet$ cross sections at the LHC, the predictions from JETPHOX multiplied by a factor close to unity for the corrections of hadronisation and underlying-event effects give a good description of the E_T^γ and p_T^{jet} measured cross sections [41, 42].

Different PDF sets are used for the calculations of these three SPS processes. MSTW2008NNLO [43] is used for $\sigma_{pp \rightarrow \gamma\gamma}^{SPS}$ calculations with 2 γ NNLO. CT10NLO [44] is used for both $\sigma_{pp \rightarrow 2jets}^{SPS}$ with NLOJet++ in fastNLO package and $\sigma_{pp \rightarrow \gamma+jet}^{SPS}$ with JETPHOX.

The calculations of $\sigma_{pp \rightarrow \gamma\gamma}^{SPS}$ are performed with the factorization and renormalization scales equal to the invariant mass of two photons, $\mu_F = \mu_R = m_{\gamma\gamma}$. The scale uncertainty and PDF uncertainty are also considered. A simplified and less computationally intensive estimate of the renormalization (μ_R) and factorization (μ_F) scale uncertainties is performed by varying these scales simultaneously by a factor of two up and down around $m_{\gamma\gamma}$, $\mu_F = \mu_R = 2m_{\gamma\gamma}$ and $\mu_F = \mu_R = 0.5m_{\gamma\gamma}$. 41 eigenvector sets of MSTW2008NNLO are used to build the PDF uncertainty envelope.

Calculations of $\sigma_{pp \rightarrow 2jets}^{SPS}$ are derived using NLOJet++ within the framework of the fastNLO package at a factorization and renormalization scale equal to the average transverse momentum (p_T^{ave}) of the two jets ($\mu_F = \mu_R = p_T^{ave}$). The uncertainty due to the choice of factorization and renormalization scales is estimated as the maximum deviation at the six points ($\mu_F/\mu, \mu_R/\mu$) = (0.5, 0.5), (2, 2), (1, 0.5), (1, 2), (0.5, 1), (2, 1) with $\mu = p_T^{ave}$. 52 eigenvector sets of CT10NLO are used to build the PDF uncertainty envelope.

For NLO calculations of $\sigma_{pp \rightarrow \gamma+jet}^{SPS}$ using JETPHOX, the renormalization, factorization and fragmentation (μ_f) scales are chosen to be photon's transverse momentum, $\mu_F = \mu_R = \mu_f = E_T^\gamma$. Same as above, 52 eigenvector sets of CT10NLO are used to build the PDF uncertainty envelope.

Above calculations were performed with the strong coupling constant at two-loop order with $\alpha_s(m_Z) = 0.118$ in CT10NLO and 0.117 in MSTW2008NNLO. The uncertainty on $\alpha_s(m_Z)$ was not considered in this study. The uncertainty from scales, pdf and $\alpha_s(m_Z)$ is around 10%, 5% and 1% respectively [25–27, 35, 36, 41, 42]. Compared to the larger uncertainty on the σ_{eff} with more than 30% used in this study as told in the end of section 2, the effect on the final results from the uncertainty on $\alpha_s(m_Z)$ can be negligible.

4 Results of $\sigma_{pp \rightarrow \gamma\gamma+2jets}^{DPS}$ and expected event rates at LHC

In this paper, several sets of typical selections at LHC were tried to calculate the production cross section of $\gamma\gamma + 2$ jets from DPS in pp collisions, $\sigma_{pp \rightarrow \gamma\gamma+2jets}^{DPS}$. Due to the high level trigger requirements for $\gamma\gamma$ events at LHC for the higher energy and higher luminosity collisions, five sets of requirements on the photons' transverse momentum were considered, $(E_T^{\gamma_1}, E_T^{\gamma_2}) > (30, 20)$ GeV, (30, 30) GeV, (40, 20) GeV, (40, 30) GeV and (40,

40) GeV with γ_1 representing the maximum E_T photon and γ_2 the minimum E_T one of two photons. So for single photon requirement in the $\gamma+jet$, 3 cases with $E_T^\gamma > (20, 30, 40)$ GeV were considered. The photon should be also constrained in the pseudorapidity region $|\eta| < 2.5$. An isolation requirement is applied on the photon to fulfill the isolation requirement from experimental measurements [25–27, 41, 42]. The standard isolation, the E_T sum of partons in a cone of size $\Delta R=0.4$ around the photon required to less than 5 GeV, is applied in JETPHOX for the calculation of $\sigma_{pp \rightarrow \gamma+jet}^{SPS}$. For 2 γ NNLO, the smooth Frixione isolation [45] on the photons is applied

$$E_T^{iso}(\Delta R) < \epsilon \left(\frac{1 - \cos(\Delta R)}{1 - \cos(\Delta R_0)} \right)^n \quad (3)$$

where $E_T^{iso}(\Delta R)$ is the E_T sum of partons in a cone of size ΔR , $\Delta R_0 = 0.4$, $\epsilon = 5$ GeV, and $n = 0.1$. This criterion is found to have the same efficiency as the standard isolation used for the other generators within a few percent [25, 26]. Additional the angular separation between two photons is required to be at least larger than 0.4 ($\Delta R_{\gamma\gamma} > 0.4$) to ensure one photon will not enter the isolation cone of the other photon, which is similar to the requirement applied in the data analyses at LHC experiments ATLAS and CMS [25–27].

In this study, jet is reconstructed with the anti- k_t clustering algorithm and cone size $R=0.5$. Jets are in the acceptance region with $|\eta^{jet}| < 4.5$. Two tries on jet p_T^{jet} were performed, $p_T^{jet} > 20$ or 25 GeV. For the dijet events, two jets should be separated by requiring their angular distance ΔR_{jj} greater than 1.0 to avoid the overlapping of two jet cones. For the $\gamma+jet$ production, the angular distance between γ and jet should be greater than 0.5 ($\Delta R_{\gamma j} > 0.5$) to ensure that the partons belong to the jet will not enter to the isolation cone of γ .

Fig. 2 shows the cross sections of $\sigma_{pp \rightarrow \gamma\gamma}^{SPS}$ computed from the 2 γ NNLO at $\sqrt{s} = 13$ TeV and 14 TeV with scales and pdf uncertainties considered, for different sets of E_T requirements on diphotons. The scale uncertainty is around 10% and the pdf uncertainty is about 4%. The selection sets in x-axis are the 5 sets of requirements on $(E_T^{\gamma_1}, E_T^{\gamma_2})$, number 1 for $(E_T^{\gamma_1}, E_T^{\gamma_2}) > (30, 20)$ GeV, 2 for $(E_T^{\gamma_1}, E_T^{\gamma_2}) > (30, 30)$ GeV, 3 for $(E_T^{\gamma_1}, E_T^{\gamma_2}) > (40, 20)$ GeV, 4 for $(E_T^{\gamma_1}, E_T^{\gamma_2}) > (40, 30)$ GeV and 5 for $(E_T^{\gamma_1}, E_T^{\gamma_2}) > (40, 40)$ GeV. The detailed values can also be found in Table 1. For the central values, the cross section with $\sqrt{s} = 14$ TeV is about 9% higher than that with $\sqrt{s} = 13$ TeV with the same selection requirements, which is within the scale and pdf uncertainties.

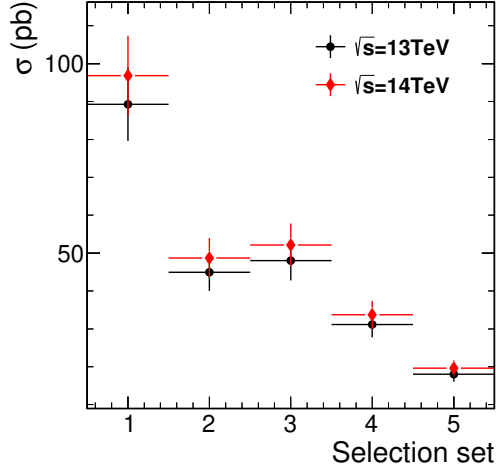


Fig. 2. Predicted cross sections of $\gamma\gamma$ by 2γ NNLO at $\sqrt{s} = 13$ TeV and 14 TeV with selection set 1 for $(E_T^{\gamma 1}, E_T^{\gamma 2}) > (30, 20)$ GeV, 2 for $(E_T^{\gamma 1}, E_T^{\gamma 2}) > (30, 30)$ GeV, 3 for $(E_T^{\gamma 1}, E_T^{\gamma 2}) > (40, 20)$ GeV, 4 for $(E_T^{\gamma 1}, E_T^{\gamma 2}) > (40, 30)$ GeV and 5 for $(E_T^{\gamma 1}, E_T^{\gamma 2}) > (40, 40)$ GeV. Scale and pdf uncertainties are included.

Table 1. Cross sections in unit of pb of $\gamma\gamma$ predicted by 2γ NNLO at $\sqrt{s} = 13$ TeV and 14 TeV. The uncertainties include the scale and pdf uncertainties.

$(E_T^{\gamma 1}, E_T^{\gamma 2}) >$	$\sqrt{s} = 13$ TeV	$\sqrt{s} = 14$ TeV
(30,20) GeV	89.3 ± 9.7	96.9 ± 10.5
(30,30) GeV	44.9 ± 4.9	48.7 ± 5.3
(40,20) GeV	48.0 ± 5.2	52.1 ± 5.7
(40,30) GeV	31.2 ± 3.4	33.7 ± 3.7
(40,40) GeV	18.0 ± 2.0	19.6 ± 2.1

Fig. 3 shows the differential cross sections, as a function of the p_T of leading jet with both jet $p_T^{jet} > 20$ GeV and $|\eta| < 4.5$, of $\sigma_{pp \rightarrow 2jets}^{SPS}$ computed from NLOJet++ within the framework of the fastNLO package at $\sqrt{s} = 13$ TeV and 14 TeV with scales and pdf uncertainties plotted in the same figure. The bottom two plots show the relative uncertainties including the scale uncertainty and scale+pdf uncertainty combined in quadrature. The contribution of pdf uncertainty is tiny. The integrated cross section are $117.6^{+4.8}_{-7.0}(\text{scale})^{+1.0}_{-1.3}(\text{pdf})$ (μb) and $122.3^{+4.6}_{-5.1}(\text{scale})^{+1.1}_{-1.4}(\text{pdf})$ (μb) for $\sqrt{s} = 13$ TeV and 14 TeV with both jet $p_T^{jet} > 20$ GeV and $|\eta^{jet}| < 4.5$, $52.2^{+1.6}_{-2.4}(\text{scale})^{+0.4}_{-0.5}(\text{pdf})$ (μb) and $56.2^{+1.8}_{-2.3}(\text{scale})^{+0.5}_{-0.6}(\text{pdf})$ (μb) for $\sqrt{s} = 13$ TeV and 14 TeV with both jet $p_T^{jet} > 25$ GeV and $|\eta^{jet}| < 4.5$. When p_T requirements on both jet increase 5 GeV from 20 GeV to 25 GeV, the cross section are reduced almost by a factor of 2.

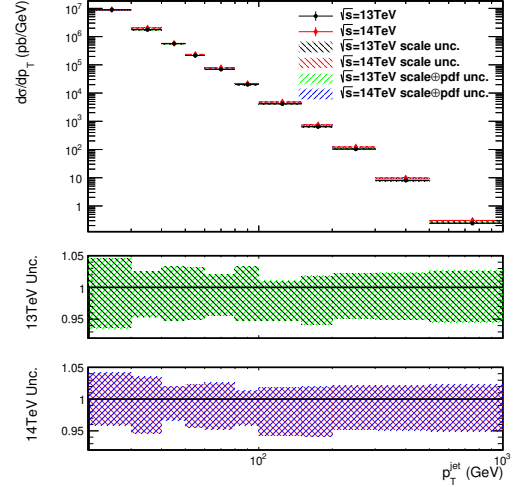


Fig. 3. Differential cross sections of $jet+jet$ computed with NLOJet++ within the framework of the fastNLO package, after the requirements on both jets with $p_T^{jet} > 20$ GeV and $|\eta^{jet}| < 4.5$. The solid black circles are the results for $\sqrt{s} = 13$ TeV while the red diamond for $\sqrt{s} = 14$ TeV. Bottom two plots show the relative uncertainties including the scale uncertainty and scale+pdf uncertainty with $\sqrt{s} = 13$ TeV in the middle plot and $\sqrt{s} = 14$ TeV in the bottom plot.

Combined the photon E_T^γ requirements for the $\gamma\gamma$ productions and the jet p_T^{jet} requirements for the $jet+jet$ productions, cross section of $\sigma_{pp \rightarrow \gamma+jet}^{SPS}$ with six sets of selections on the transverse momentums of photon and jet with $(E_T^\gamma, p_T^{jet}) > (20, 20)$ GeV, $(30, 20)$ GeV, $(40, 20)$ GeV, $(20, 25)$ GeV, $(30, 25)$ GeV and $(40, 25)$ GeV were calculated. Fig. 4 shows the differential cross sections of $\sigma_{pp \rightarrow \gamma+jet}^{SPS}$ as a function of photon E_T^γ with $(E_T^\gamma, p_T^{jet}) > (40, 20)$ GeV, $|\eta^\gamma| < 2.5$, $|\eta^{jet}| < 4.5$ and separation $\Delta R_{\gamma j} > 0.5$, computed from JETPHOX with $\sqrt{s} = 14$ TeV. The contributions from the direct photon production and photon from fragmentation are shown in the same plot. The scales and pdf uncertainties are also plotted in the same figure. The integrated cross sections are listed in Table 2 for different sets of selections and collision energies. The scale and pdf uncertainties are also listed in this table, with about 10% uncertainty from scales and around 4% from pdf.

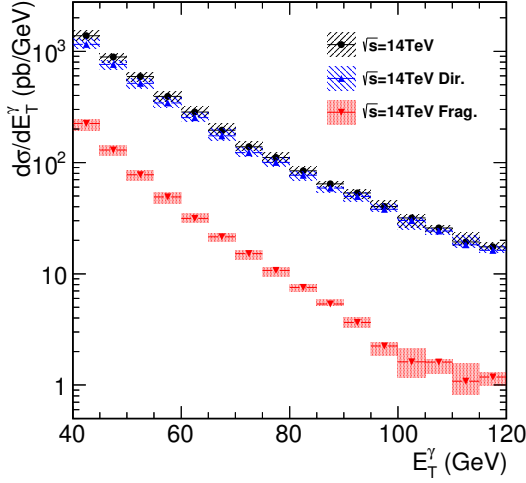


Fig. 4. Differential cross sections of $\gamma + jet$ as a function of the photon E_T^γ , computed with JETPHOX and the selections $(E_T^\gamma, p_T^{jet}) > (40, 20)$ GeV, $|\eta^\gamma| < 2.5$, $|\eta^{jet}| < 4.5$ and separation $\Delta R_{\gamma j} > 0.5$ at $\sqrt{s} = 14$ TeV. The solid circle are the total contributions while the blue triangles represent the direct contribution and the red triangles are the contributions of photon from fragmentation. Scales and pdf uncertainties are also shown in this plot.

Table 2. Cross sections in unit of 10^3 pb of $\gamma + jet$ predicted by JETPHOX at $\sqrt{s} = 13$ TeV and 14 TeV. The total uncertainties including scale uncertainty and pdf uncertainty are also list in this table.

$(E_T^\gamma, p_T^{jet}) >$	$\sqrt{s} = 13$ TeV	$\sqrt{s} = 14$ TeV
(20,20) GeV	$90.1^{+11.0}_{-9.6}$	$97.2^{+13.3}_{-11.6}$
(30,20) GeV	$48.7^{+5.2}_{-4.6}$	$52.7^{+5.7}_{-5.0}$
(40,20) GeV	$20.2^{+2.2}_{-1.8}$	$22.0^{+2.5}_{-2.1}$
(20,25) GeV	$85.0^{+9.8}_{-8.7}$	$91.7^{+10.9}_{-9.1}$
(30,25) GeV	$41.5^{+4.4}_{-3.9}$	$45.0^{+4.7}_{-4.4}$
(40,25) GeV	$19.7^{+2.0}_{-1.8}$	$21.4^{+2.4}_{-1.9}$

According to Eq.2 and the above cross sections of the SPS processes, the cross sections for the production of pairs of photons plus two additional jets produced from double parton scattering (DPS) in high-energy proton-proton collisions at the LHC are calculated for the first time. The results are summarized in Table 3. Two jets in the same $pp \rightarrow \gamma\gamma + 2jets$ event from DPS have the same p_T cut thresholds, both $p_T^{jet} > 20$ GeV or 25 GeV simultaneously. The calculated cross section can be around 0.1 pb to ≈ 1 pb with the selections considered in this paper. The uncertainty on the cross section is around 50%, with the dominant contribution from the uncertainty of σ_{eff} .

Table 3. Cross sections in unit of pb of $\sigma_{pp \rightarrow \gamma\gamma + 2jets}^{DPS}$ calculated for $\sqrt{s} = 13$ TeV and

14 TeV with the selections described in the paper. The total uncertainties including scale uncertainty, pdf uncertainty and also the σ_{eff} uncertainty are also list in this table.

$(E_T^{\gamma_1}, E_T^{\gamma_2}, \text{both } p_T^{jet}) >$	$\sqrt{s} = 13$ TeV	$\sqrt{s} = 14$ TeV
(30,20,20) GeV	$0.846^{+0.423}_{-0.432}$	$0.960^{+0.481}_{-0.479}$
(30,20,25) GeV	$0.428^{+0.213}_{-0.215}$	$0.500^{+0.250}_{-0.250}$
(30,30,20) GeV	$0.431^{+0.215}_{-0.219}$	$0.489^{+0.243}_{-0.242}$
(30,30,25) GeV	$0.428^{+0.213}_{-0.215}$	$0.250^{+0.124}_{-0.124}$
(40,20,20) GeV	$0.437^{+0.218}_{-0.222}$	$0.496^{+0.247}_{-0.247}$
(40,20,25) GeV	$0.223^{+0.113}_{-0.111}$	$0.261^{+0.130}_{-0.129}$
(40,30,20) GeV	$0.277^{+0.137}_{-0.141}$	$0.313^{+0.155}_{-0.155}$
(40,30,25) GeV	$0.136^{+0.068}_{-0.067}$	$0.159^{+0.078}_{-0.078}$
(40,40,20) GeV	$0.154^{+0.076}_{-0.079}$	$0.176^{+0.086}_{-0.087}$
(40,40,25) GeV	$0.076^{+0.038}_{-0.037}$	$0.089^{+0.044}_{-0.043}$

With an integrated luminosity of 100 fb^{-1} at $\sqrt{s} = 13$ TeV accumulated in the following years, about 85k $pp \rightarrow \gamma\gamma + 2jets$ events from DPS can be obtained with the loosest selections, diphoton $(E_T^{\gamma_1}, E_T^{\gamma_2}) > (30, 20)$ GeV and both jets $p_T^{jet} > 20$ GeV. These events can be triggered by the diphoton paths proposed at the LHC for $\sqrt{s} = 13$ TeV. When the integrated luminosity increasing at $\sqrt{s} = 14$ TeV, tighter E_T thresholds on diphoton for the trigger will be used. With the tighter selections, diphoton $(E_T^{\gamma_1}, E_T^{\gamma_2}) > (40, 30)$ GeV and both jets $p_T^{jet} > 20$ GeV, about 940k $pp \rightarrow \gamma\gamma + 2jets$ events from DPS can be obtained with an integrated luminosity of 3000 fb^{-1} . Even with the tightest selections studied in this paper, diphoton $(E_T^{\gamma_1}, E_T^{\gamma_2}) > (40, 40)$ GeV and both jets $p_T^{jet} > 25$ GeV, we can also get about 260k $pp \rightarrow \gamma\gamma + 2jets$ events from DPS with 3000 fb^{-1} as designed by LHC.

5 Summary and outlook

In this paper, the cross sections for the production of pairs of photons plus two additional jets produced from double parton scattering in high-energy proton-proton collisions at the LHC with $\sqrt{s} = 13$ TeV and 14 TeV (LHC Run2) are calculated for the first time. With the generic formula, the cross sections have been computed based on the theoretical perturbative QCD predictions for the productions of $\gamma\gamma$ at next-to-next-to-leading-order, jet + jet and $\gamma + jet$ at next-to-leading-order, with their corresponding single-scattering cross sections. From the LHC measurements with the collision data obtained in years 2011 and 2012 (LHC Run1), these theoretical predictions for these three SPS processes can give the best agreements with the measured data. With the typical acceptance and selections used at LHC, the cross sections $\sigma_{pp \rightarrow \gamma\gamma + 2jets}^{DPS}$ can be estimated to be around 0.1 pb to 1 pb with the collision energy $\sqrt{s} = 13$ TeV or 14 TeV. The expected event rates for $\gamma\gamma + 2jets$ from DPS, with some sets of selections, are given for proton-proton collisions with the collision energy $\sqrt{s} = 13$ TeV

and an integrated luminosity of 100 fb^{-1} planned for the following two years, and also $\sqrt{s} = 14 \text{ TeV}$ with 3000 fb^{-1} of integrated luminosity as LHC designed. The uncertainties on the cross section and the events rates are mainly dominated by the σ_{eff} uncertainty. The scale and pdf uncertainties for the productions of these three SPS processes are also considered.

With the incoming LHC Run2 data, there are enough $pp \rightarrow \gamma\gamma + 2jets$ events from DPS for investigations. It needs further studies on the variables, such as the angles

between two photons and two jets, to be chosen for the discrimination of $pp \rightarrow \gamma\gamma + 2jets$ events from DPS and $pp \rightarrow \gamma\gamma + 2jets$ events from SPS when performing the data analysis. Also the contributions from the DPS to the whole $pp \rightarrow \gamma\gamma + 2jets$ event rates on the distributions of some typical variables are need detailed investigations in the LHC Run2 data analysis.

The authors would like to thank Dr. Hua-Sheng Shao from CERN for helpful discussions.

References

- 1 Landshoff P V and Polkinghorne J C. Phys. Rev. D, 1978, **18**: 3344
- 2 Lansberg J P and Shao H S. arXiv:hepph/1410.8822
- 3 ATLAS collaboration. New J. Phys., 2013, **15**: 033038
- 4 CMS collaboration. J. High Energy Phys., 2014, **1403**: 032
- 5 ATLAS collaboration. J. High Energy Phys., 2014, **1405**: 068
- 6 UA2 collaboration. Phys. Lett. B, 1991, **268**: 145
- 7 AFS collaboration. Z. Phys. C, 1987, **34**: 163
- 8 CDF collaboration. Phys. Lett. D, 1993, **47**: 4857
- 9 CDF collaboration. Phys. Lett. D, 1997, **56**: 3811
- 10 CDF collaboration. Phys. Lett. D, 2010, **81**: 052012
- 11 Diehl M, Ostermeier D and Schafer A. J. High Energy Phys., 2012, **03**: 089
- 12 Calucci G and Treleani D. Phys. Rev. D, 2011, **83**: 016012
- 13 Fabbro A D and Treleani D. Phys. Rev. D, 2000, **61**: 077502
- 14 Hussein M. Nucl. Phys. Proc. Suppl., 2007, **174**: 55
- 15 Bandurin D, Golovanov G and Skachkov N. J. High Energy Phys., 2011, **04**: 054
- 16 Mekhfi M. Phys. Rev. D, 1985, **32**: 2371
- 17 Ametller L, Paver N and Treleani D. Phys. Lett. B, 1986, **169**: 289
- 18 Gaunt J R, Kom C H, Kulesza A and Stirling W J. Eur. Phys. J. C, 2010, **69**: 53
- 19 CMS Collaboration. Phys. Lett. B, 2012, **716**: 30
- 20 ATLAS Collaboration. Phys. Lett. B, 2012, **716**: 1
- 21 ATLAS collaboration. Phys. Lett. B, 2012 **718**: 411
- 22 ATLAS collaboration. New J. Phys., 2013, **15**: 043007
- 23 CMS collaboration. Phys. Lett. B, 2013, **719**: 42
- 24 CMS collaboration. J. High Energy Phys., 2013, **03**: 111
- 25 CMS collaboration. Eur. Phys. J. C, 2014, **74**: 3129
- 26 Tao J. Nucl. Part. Phys. Proc., 2015, **258-259**: 7-10
- 27 ATLAS collaboration. Phys. Rev. D, 2012, **85**: 012003
- 28 Enterria D and Snigirev A M. Nucl. Phys. A, 2014, **931**: 303-308
- 29 Bahr M, Myska M, Seymour M H and Siodmok A. J. High Energy Phys., 2013, **03**: 129
- 30 Binoth T, Guillet J, Pilon E and Werlen M. Eur. Phys. J. C, 2000, **16**: 311
- 31 Bern Z, Dixon L J and Schmidt C. Phys. Rev. D, 2002, **66**: 074018
- 32 Balazs C, Nadolsky P M, Schmidt C and Yuan C P. Phys. Lett. B, 2000, **489**: 157
- 33 Balazs C, Berger E L, Nadolsky P M and Yuan C P. Phys. Lett. B, 2006, **637**: 235
- 34 Catani S, Cieri L, Florian D, Ferrera G and Grazzini M. Phys. Rev. Lett., 2012, **108**: 072001
- 35 ATLAS collaboration. J. High Energy Phys., 2014, **05**: 059
- 36 CMS collaboration. Phys. Lett. B, 2011, **700**: 187; CMS collaboration. Eur. Phys. J. C, 2013, **73**: 2604; CMS collaboration. Phys. Rev. D, 2013, **87**: 112002; CMS collaboration. 2014, CMS-PAS-SMP-14-002
- 37 Nagy Z. Phys. Rev. D, 2003, **68**: 094002
- 38 Cacciari M, Salam G P and Soyez G. J. High Energy Phys., 2008, **04**: 063
- 39 Kluge T, Rabbertz K and Wobisch M. arXiv:hep-ph/0609285v2
- 40 Catani S, Fontannaz M, Guillet J P and Pilon E. J. High Energy Phys., 2002, **05**: 028
- 41 ATLAS collaboration. Nucl. Phys. B, 2013, **875**: 483-535
- 42 CMS collaboration. Phys. Rev. Lett., 2011, **106**: 082001
- 43 Martin A D, Stirling W J, Thorne R S and Watt G. Eur. Phys. J. C, 2009, **63**: 189-285
- 44 Lai H L et al. Phys. Rev. D, 2010, **82**: 074024
- 45 Frixiene S. Phys. Lett. B, 1998, **429**: 369